Canadian Precipitation Patterns Associated with the Southern Oscillation

AMIR SHABBAR, BARRIE BONSAL, AND MADHAV KHANDEKAR

Atmospheric Environment Service, Environment Canada, Downsview, Ontario, Canada

(Manuscript received 14 January 1997, in final form 2 May 1997)

ABSTRACT

Precipitation responses over Canada associated with the two extreme phases of the Southern Oscillation (SO), namely El Niño and La Niña, are identified. Using the best available precipitation data from 1911 to 1994, both the spatial and temporal behavior of the responses are analyzed from the El Niño/La Niña onset to several seasons afterward. Composite and correlation analyses indicate that precipitation over a large region of southern Canada extending from British Columbia, through the prairies, and into the Great Lakes region is significantly influenced by the SO phenomenon. The results show a distinct pattern of negative (positive) precipitation anomalies in this region during the first winter following the onset of El Niño (La Niña) events. During this same period, significant positive precipitation anomalies occur over the northern prairies and southeastern Northwest Territories in association with El Niño events. Statistical significance of the responses is tested by the Student's t-test and the Wilcoxon rank-sum test, while field significance is established through the Monte Carlo procedure. All of the significant precipitation anomalies can be explained by the associated upper-atmospheric flow patterns, which during the first winter following the onset of El Niño (La Niña) events resemble the positive (negative) phase of the Pacific–North American (PNA) pattern. Significant correlations between Southern Oscillation index (SOI) values and the observed precipitation anomalies over southern Canada suggest the possibility of developing a long-range forecasting technique for Canadian precipitation based on the occurrence and evolution of the various phases of the SO.

1. Introduction

In Canada, many economic activities and environmental processes are highly dependent on precipitation. Occurrences of large-scale precipitation deficits often have severe effects on activities such as agriculture, forestry, hydroelectric production, wetlands, and wildlife. For example, it was estimated that the 1988 drought, which adversely affected the grain-growing areas of both Canada and the United States, cost the Canadian economy approximately $1.8 billion in terms of decreased agricultural and hydroelectric production, increased forest fires, and loss of habitat for waterfowl and wildlife (Wheaton et al. 1992). Occurrences of large-scale precipitation surpluses are often beneficial to the aforementioned activities. However, a persistence of anomalously wet conditions can also have severe effects (e.g., flooding, snow removal, delays in harvesting, and others).

Due to Canada's large expanse [which covers several climatic zones (Hare and Thomas 1974)], there are wide spatial and temporal variations in mean annual precipitation (Fig. 1). The Pacific coast is the wettest region with mean annual values approaching 3000 mm. The majority of this precipitation is received during winter. Precipitation quickly decreases in the interior of British Columbia due to the rainshadow effects of the west coast mountains. A second precipitation maximum occurs in eastern Canada. Amounts are highest along the East Coast and decrease westward at a rate of approximately 40 mm every 100 km (Philips 1990). Over most of eastern Canada, precipitation is evenly distributed throughout the year. Between these two maxima, smaller annual totals are found, with lowest values on the southern prairies (less than 500 mm). The lower amounts are essentially the result of the prairies' location in the lee of the Rocky Mountains and their distance from large moisture sources. The driest regions of the country occur over northern Canada and the high Arctic, mainly due to the dominance of cold air and the lack of any large moisture sources. Values range from near 400 mm in more southerly locations, to less than 200 mm in the high Arctic islands. The prairies receive the majority of their precipitation during late spring and summer, and Arctic Canada, during late summer and early autumn (Hare and Thomas 1974; Philips 1990). Within these spatial and temporal patterns, there is also considerable interannual variability. The ability to obtain a better understanding of the potential causes of this variability, may aid in the prediction of large-scale precipitation anomalies.

Corresponding author address: Dr. Barrie Bonsal, Atmospheric Environment Services (CCRM), 4905 Dufferin Street, Downsview, ON M3H 5T4, Canada.
E-mail: barrie.bonsal@ec.gc.ca

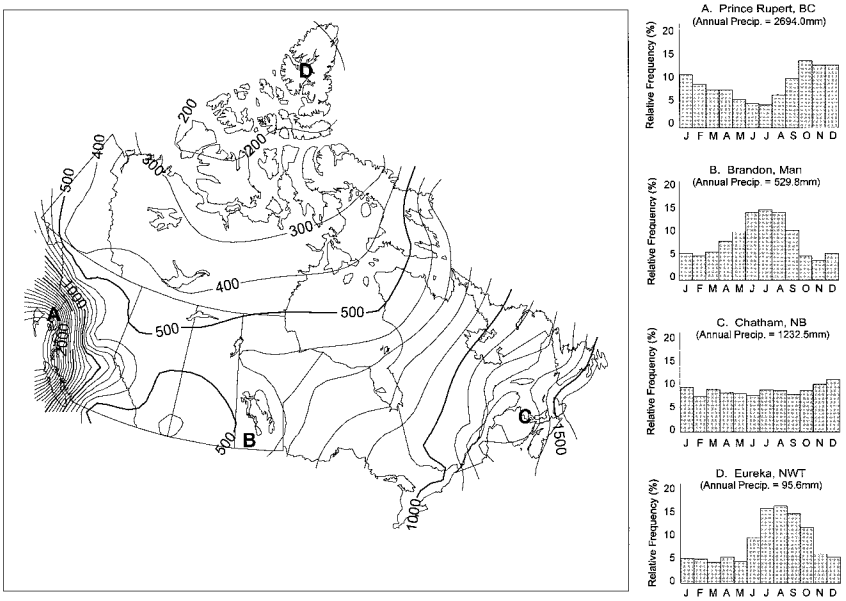

FIG. 1. Mean annual precipitation (mm) over Canada (1961–90). Contour interval is 100 mm. Histograms on the right show the monthly relative frequency (%) of annual precipitation for selected stations as identified by letters on the map.

Recently, there have been several investigations into possible relationships between the different phases of the Southern Oscillation (SO) and interannual climatic variability over various regions of the world. These have ranged from global-scale (e.g., Ropelewski and Halpert 1987, 1989; Kiladis and Diaz 1989) to regional-scale studies in both the Tropics (e.g., McBride and Nicholls 1983; Khandekar and Neralla 1984; Rogers 1988) and extratropics (e.g., Yarnal and Diaz 1986; Bunkers et al. 1996; Shabbar and Khandekar 1996). Generally, over North America, above-normal precipitation was observed from October of the El Niño onset year [i.e., October of year 0, denoted as Oct(0)] through the following March [i.e., March of year +1 with respect to the onset, denoted as Mar(+1)] over the southeastern United States and northern Mexico. Above-normal amounts were also found in the Great Basin region of the western United States during Apr(0) through Oct(0) (Ropelewski and Halpert 1986, 1987, 1989; Halpert and Ropelewski 1992). In association with La Niña events, winter(+1) often had below normal precipitation over the southeastern United States (Kiladis and Diaz 1989). More regionally, Bunkers et al. (1996) determined that on the northern plains of the United States, Apr(0) to Oct(0) of El Niño years showed an increase in mean precipitation, while the May(0) to Aug(0) period associated with La Niña events had an opposite response. In a temperature study done specifically for Canada, Shabbar and Khandekar (1996) found that for El Niño, significant positive temperature anomalies spread eastward from the west coast of Canada to the Labrador coast during the late autumn to early spring following the onset of the events. Significant negative anomalies spread southeastward from the Yukon and extended into the upper Great Lakes region by the winter season following the onset of La Niña events.

In all the previous studies, the observed temperature and precipitation anomalies during winter(+1) have mainly been attributed to the upper-atmospheric circulation anomalies associated with the different phases of the SO. In particular, during El Niño (La Niña), the positive (negative) phase of the Pacific–North American (PNA) pattern is often observed during the winter following the onset of the events (e.g., Horel and Wallace 1981; Yarnal and Diaz 1986). The pressure anomalies associated with the different phases of the PNA alter the normal upper-atmospheric flow patterns, thus affecting temperature and precipitation patterns over various regions of North America.

Even though several studies have examined temperature and precipitation patterns associated with the SO, none have specifically focused on Canadian precipitation. The purpose of this investigation is to identify coherent precipitation signals over Canada associated with the two extreme phases of the SO (i.e., El Niño and La Niña). Using a comprehensive Canadian precipitation dataset, both the spatial and temporal behavior of the precipitation responses are examined from the El Niño/La Niña onset to several seasons afterward. Significance of the results is established by the Student's t-test and the nonparametric Wilcoxon rank-sum test. Additionally, the precipitation anomalies are linked to observed changes in upper atmospheric flow patterns. The data and methodology for this analysis are discussed in section 2, and the results presented in section 3. A discussion of these results, along with a summary

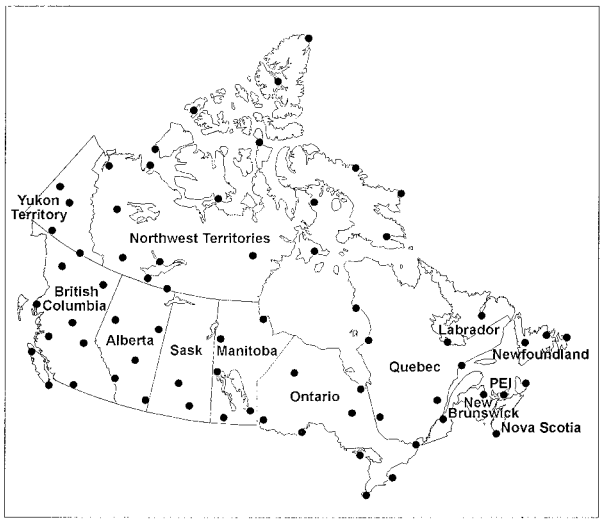

FIG. 2. Location of precipitation stations used in this study. Station names are given in Table 2.

and concluding remarks, are provided in sections 4 and 5 respectively.

2. Data and methodology

a. Data

The precipitation data include monthly values for the 69 stations shown in Fig. 2 and Table 1. They are based on corrected daily rain and snow measurements. This includes corrections for missing values, instrument changes, wind undercatch, evaporation, wetting loss, and trace events. The trace adjustment is quite important especially in northern Canada, where precipitation is low and many trace events are recorded. As a result, this is the best long-term dataset currently available for Canadian precipitation (Mekis and Hogg 1996). The majority of the data for southern areas are from 1911 to 1994. Many of the higher latitude stations have shorter records. A list of the stations, along with their period of record, are given in Table 1. The number of El Niño and La Niña events occurring in this record is also provided.

Three-month running seasons are used for the precipitation analysis. There are 12 running seasons for each year, starting with January–March (JFM) and ending with December–February (DJF). Seasonal precipitation values are determined by averaging the 3-monthly values within each season. The amounts are then standardized by subtracting the average seasonal value (for the entire period of record) from the actual value and dividing by the standard deviation. These standardized anomalies form the basis for further analysis.

Upper-atmospheric data consist of monthly (1200 UTC) 500-hPa height analyses of the Northern Hemisphere (15°–90°N) for the period 1946–94 as outlined by Shabbar and Khandekar (1996). Upper-atmospheric anomalies are calculated relative to the 49-yr base period. Monthly standardized Southern Oscillation index (SOI) data from 1911 to 1994 were obtained from the U.S. Department of Commerce, National Oceanic and Atmospheric Administration (NOAA), Climate Prediction Center in Washington, D.C. Seasonal SOI values are determined by averaging the 3-monthly values within each season.

Individual El Niño and La Niña events are the same as those used by Rasmusson (1984), Ropelewski and Jones (1987), Halpert and Ropelewski (1992), and Shabbar and Khandekar (1996). Strong to moderate El Niño (La Niña) events were defined as those years in which the 5-month running mean SOI remained in the lower (upper) 25% of the distribution for 5 months or longer. For the period of 1911–94, this results in 22 El Niño and 14 La Niña years (Table 2). When El Niño and La Niña episodes occurred in consecutive years (e.g., 1975 and 1976), or when an event spanned more than 1 yr (e.g., 1957 and 1958 El Niño), the analysis treated these as separate episodes.

b. Methodology

The initial step is to construct seasonal precipitation composite maps for both El Niño and La Niña events and identify regions within Canada that show significant responses. Typical El Niño and La Niña events tend to develop during summer to early autumn, mature during winter, and terminate during the following spring (Rasmusson and Carpenter 1982; Kiladis and Diaz 1989). To identify all possible precipitation-related impacts associated with these events, composites are formed from the beginning of the onset year [JFM(0)] to the end of the second year following the onset [OND(+2)] (a 3-yr period). Two statistical tests are used to determine local significant differences in mean standardized precipitation between El Niño and non-SO (i.e., non–El Niño and non–La Niña) periods, and La Niña and non-SO periods. The first is the standard two-tailed Student's t-test (e.g., Norman and Streiner 1986). The nonparametric Wilcoxon rank-sum test (Bethea et al. 1995) is also used (see the appendix) and compared with the results of the Student's t-test. Field significance (Livezey and Chen 1983) of the composite maps is evaluated through a Monte Carlo procedure. For each season, the El Niño/La Niña years are randomly shuffled (10 000 times) and a mean t statistic for the 69 stations is calculated. The number of times the mean of the t statistic generated by the random simulations exceeds that of the actual t value is determined and assessed at the 5% significance level.

The precipitation field over Canada generally exhibits large natural variability (Shabbar 1993). Since this study attempts to extract SO-related influences, a correlation analysis relating precipitation to the SOI is also carried out. This procedure aids in reinforcing or confirming the results of the composite analysis. The DJF SOI val-

TABLE 1. Precipitation stations used in this study. Geographical locations are given in Fig. 2.

Station name	Period of record	Number of El Niño events	Number of La Niña events
British Columbia			
Victoria	1911–94	22	14
Quatsino	1911–94	22	14
Bella Coola	1911–94	22	14
Prince Rupert	1911–94	22	14
Barkerville	1911–94	22	14
Fort St. James	1911–94	22	14
Princeton	1911–94	22	14
Fort Nelson	1937–94	13	10
Dease Lake	1944–94	11	9
Alberta			
Banff	1911–94	22	14
Medicine Hat	1911–94	22	14
Edmonton	1911–94	22	14
Fairview	1931–91	13	10
Fort McMurray	1944–94	11	9
Saskatchewan			
Regina	1911–94	22	14
Saskatoon	1911–93	22	14
Manitoba			
Brandon	1911–94	22	14
Great Falls	1922–94	17	12
The Pas	1911–94	22	14
Lynn Lake	1948–94	11	9
Churchill	1929–94	15	10
Ontario			
Kenora	1911–94	22	14
Thunder Bay	1911–93	22	14
Gore Bay	1915–93	19	14
Harrow	1917–91	19	13
Welland	1911–94	22	14
Ottawa	1911–94	22	14
Big Trout Lake	1939–92	13	9
Moosonee	1911–93	22	14
Kapuskasing	1918–94	19	12
Quebec			
Amos	1913–94	20	14
Quebec City	1911–94	22	14
Chicoutimi	1911–94	22	14
Nitchequon	1942–94	11	9
Sept-Iles	1944–94	11	9
Inukjuak	1933–93	13	10
Kuujjuaq	1947–94	11	9
Kuujjuarapik	1925–94	17	11
New Brunswick			
Chatham	1911–94	22	14
Nova Scotia			
Yarmouth	1911–94	22	14
Sydney	1911–94	22	14
Prince Edward Island			
Charlottetown	1911–92	22	14
Newfoundland and Labrador			
St. John's	1911–94	22	14
Deer Lake	1933–94	13	10
Gander	1937–94	13	10
Goose	1941–94	12	9
Yukon Territory			
Dawson	1911–94	22	14
Mayo	1925–94	17	11
Watson Lake	1938–93	13	10
Whitehorse	1942–94	11	9
Northwest Territories			
Fort Simpson	1911–94	22	14
Hay River	1911–94	22	14
Norman Wells	1911–94	22	14
Inuvik	1926–94	16	11
Fort Smith	1943–94	11	9
Yellowknife	1942–94	11	9
Baker Lake	1949–94	11	9
Cambridge Bay	1940–94	12	9
Coral Harbour	1945–94	11	9
Hall Beach	1957–94	9	6
Mould Bay	1948–94	11	9
Resolute	1947–94	11	9
Sachs Harbour	1955–94	9	8
Cape Dyer	1959–93	7	6
Alert	1950–94	11	9
Clyde	1946–94	11	9
Eureka	1948–94	11	9
Iqaluit	1946–94	11	9
Cape Parry	1957–93	9	6

ues are correlated with seasonal precipitation for the same periods as the composite analysis. The SOI values for DJF are used because they tend to be associated with the mature stages of El Niño and La Niña events (e.g., Rasmusson and Carpenter 1982; Philander 1990). The significance of the correlation analysis is also tested through a Monte Carlo procedure. For each station and season, the precipitation time series is randomly shuffled 10 000 times and correlated with the SOI time series to produce a random distribution of correlation coefficients. The original correlation values are compared to this empirically derived distribution to assess their statistical significance at the 5% level.

3. Results

a. Winter(+1) precipitation over southern Canada

1) COMPOSITE ANALYSIS

Composite standardized precipitation anomalies for both El Niño and La Niña are mapped and statistically analyzed from JFM(0) to OND(+2). The strongest results (i.e., several significant stations over a coherent region) occur during the winter following the onset of both El Niño and La Niña over a region that encompasses a large portion of southern Canada, extending from approximately British Columbia to the Ontario–Quebec border. The season that displays the highest field significance for both events is JFM(+1), the period that

TABLE 2a. Years of onset of strong to moderate El Niño events. During these events, the SOI remained in the lower 25% of the distribution for 5 months or longer (after Rasmusson 1984).

1911–19	1920–29	1930–39	1940–49	1950–59	1960–69	1970–79	1980–89	1990–94
1911	1925	1930	1941	1951	1965	1972	1982	1991
1912	1926	1939		1953	1969	1976	1986	
1914	1929			1957				
1918				1958				
1919								

also typically coincides with the mature stages of SO-related events (Figs. 3a,b). Shading denotes areas in which individual stations are statistically significant. For almost all of these stations, both the Student's t-test and Wilcoxon rank-sum test show statistical significance, thus reinforcing the robustness of the results.

During the JFM(+1) season of El Niño episodes, significant negative values stretch from southern British Columbia, across the southern prairies, and into the western Great Lakes region. The pattern begins to emerge during NDJ(+1). The anomalies are strongest and cover the largest area during DJF(+1) and JFM(+1). In FMA(+1), they weaken and are mainly confined to southern British Columbia and Alberta (not shown). By MAM(+1), no significant anomaly is found in this region. Figure 3a also shows significant positive anomalies over the northern prairies and southeastern Northwest Territories. This region, defined here as ''north-central Canada,'' is discussed in section 3b. Recently, Shabbar and Barnston (1996) employed the canonical correlation analysis (CCA) technique to examine the skill of seasonal temperature and precipitation forecasts in Canada. Their leading CCA loading pattern for winter precipitation shows a dipole pattern that is very similar to the precipitation anomaly pattern shown in Fig. 3a (see their Fig. 18). They indicated that the warm phase of the SO plays a dominant role in these Canadian precipitation anomalies during winter.

Figure 3b shows the precipitation pattern during JFM(+1) of La Niña episodes. Significant positive precipitation anomalies cover most of interior British Columbia and Alberta. They weaken (but remain significant) through south-central Saskatchewan and Manitoba and strengthen again over northwestern Ontario and into the Great Lakes–St. Lawrence region. As with El Niño, the pattern emerges during NDJ(+1), is strongest during DJF(+1) and JFM(+1), then weakens and disappears through FMA(+1) and MAM(+1). Figure 3b also suggests a positive precipitation anomaly response over portions of the northwestern Arctic. However, this region does not show statistical significance and, therefore, is not further discussed.

A comparison of Figs. 3a and 3b reveals that significant opposite responses over the southern portions of Canada do not occur in exactly the same area. During the La Niña winters, significant precipitation anomalies cover larger portions of British Columbia and Alberta, and extend farther eastward into southern Quebec. Furthermore, significant positive precipitation responses associated with El Niño occur over north-central Canada. This indicates that stations with significant precipitation anomalies do not necessarily exhibit opposite responses to the two phases of the SO. Nonetheless, there is a large area of southern Canada that is affected by both phases and shows an opposite response. The remainder of section 3a examines this region in more detail. For this investigation, ''southern Canada'' is defined as the intersection of significant areas shown in Figs. 3a,b. Precipitation values for all the stations within this region are averaged and further analyzed.

The evolution of composite areally averaged precipitation anomalies over southern Canada associated with El Niño and La Niña events is shown in Fig. 4. The time series clearly shows the strongest response occurring during the winter following the onset of the events with both curves peaking during the DJF(+1) to JFM(+1) period. During the El Niño phase, the standardized anomaly reaches −0.42, and for La Niña, the values peak at +0.54. Following this, the values weaken considerably and change sign.

2) VARIABILITY

The variability in winter(+1) precipitation over southern Canada is examined by comparing the distributions of JFM(+1) precipitation associated with El Niño, La Niña, and non-SO seasons (Fig. 5). The actual (as opposed to standardized) anomalies are used to provide an indication of the magnitude of the responses. On average, El Niño events are associated with negative anomalies and La Niña with positive anomalies. However, there is substantial variability about the mean in the three distributions. For example, some El Niño events are associated with positive precipitation anomalies, while some La Niña have negative anomalies. This is likely attributable to other factors influencing winter precipitation over southern Canada, or to variations within each El Niño/La Niña event itself. Nonetheless, there is a significant difference in mean precipitation between SO and non-SO episodes.

Table 3 further quantifies the relationship based on shifts in the JFM(+1) precipitation distribution associated with individual El Niño and La Niña episodes. The top portion gives the precipitation anomaly category in which individual El Niño and La Niña events occur. Negative anomalies occur during 20 of the 22 El

TABLE 2b. Years of onset of strong to moderate La Niña events. During these events, the SOI remained in the upper 25% of the distribution for 5 months or longer (after Ropelewski and Jones 1987).

1911–19	1920–29	1930–39	1940–49	1950–59	1960–69	1970–79	1980–89	1990–94
1916	1924	1938	—	1950	1964	1970	1988	—
1917	1928			1955		1971		
				1956		1973		
						1975		

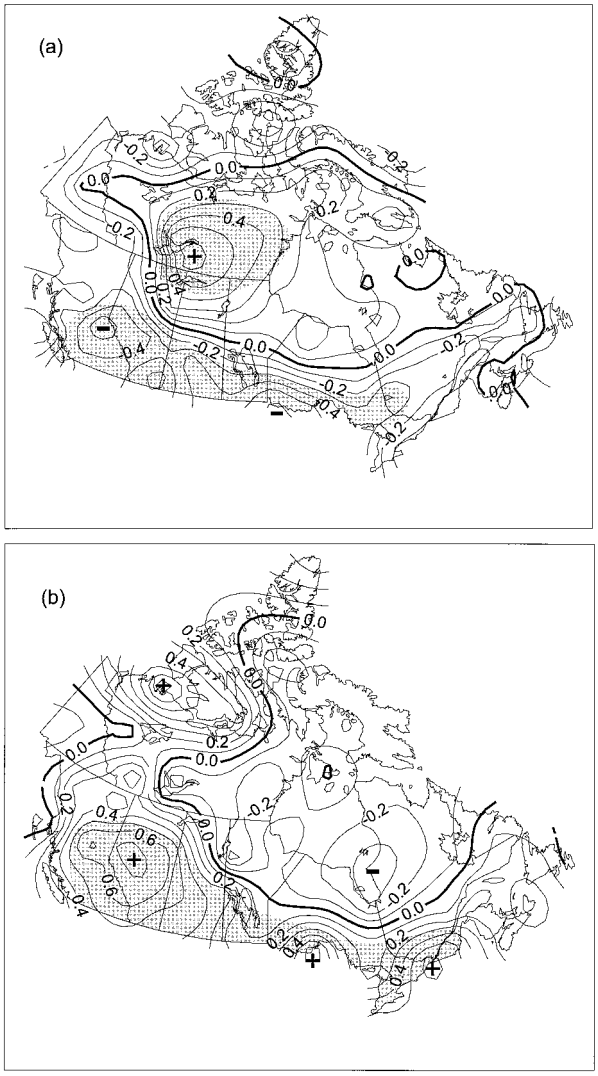

FIG. 3. (a) Composite of standardized precipitation anomalies for the JFM season following the onset of El Niño events [JFM(+1)]. Contour interval is 0.1. Shading denotes areas with precipitation anomalies significantly different from non-SO (non–El Niño and non–La Niña) periods using the Student's t-test and Wilcoxon rank-sum test (5% level). The map shows field significance at the 1% level as determined by the Monte Carlo procedure described in section 2b. (b) Same as (a) but following the onset of La Niña events. The map shows field significance at the 1% level.

Niño events. The majority of these seasons are associated with anomalies between 0 and −5 mm. For La Niña, 10 of the 14 events are associated with positive anomalies, with the majority falling between 0 and 15 mm. The remainder of Table 3 lists the driest and wettest 10% of all JFMs on record along with the type of associated event. Six of the eight driest seasons are associated with El Niño, including the driest winter of 1912. The association for La Niña is not as strong, although two of the three wettest seasons are associated with these events (including the wettest winter of 1972). Table 3 also highlights inter-SO precipitation variability. However, many of the driest winter seasons are associated with El Niño events. This is significant since extreme dry winter conditions often have adverse effects on runoff and soil moisture recharge during the following spring, which can be quite critical to many economic activities over southern Canada (e.g., agriculture).

3) CORRELATION ANALYSIS

To better understand the tropical influences on Canadian precipitation, DJF SOI values are correlated with seasonal standardized precipitation anomalies over Can-

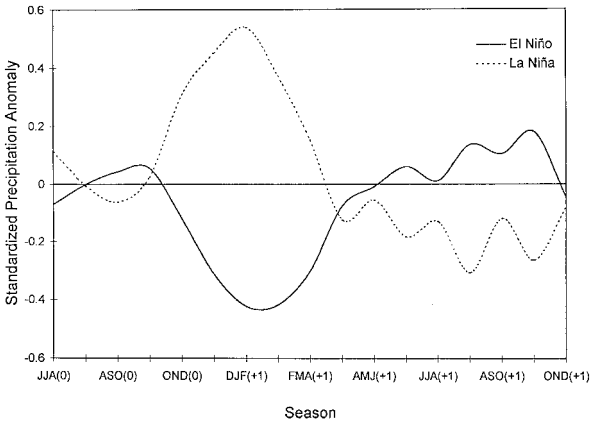

FIG. 4. Seasonal march of the areally averaged composite standardized precipitation anomalies over southern Canada from JJA of the El Niño/La Niña onset year [JJA(0)] to OND of year +1 with respect to the onset [OND(+1)]. El Niño (solid) and La Niña (dashed). See text for definition of southern Canada.

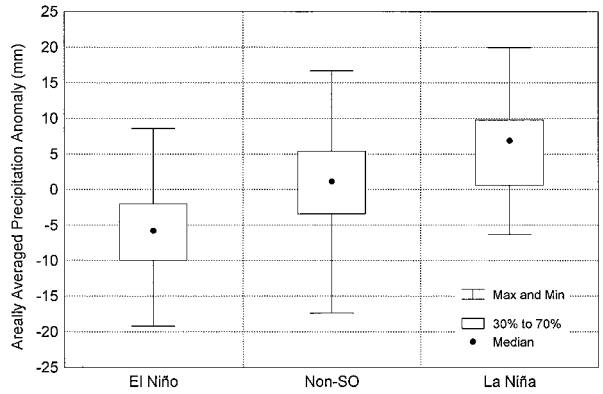

FIG. 5. Box plot comparing the JFM(+1) precipitation distribution for southern Canada associated with El Niño, La Niña, and non-SO (non–El Niño and non–La Niña) periods.

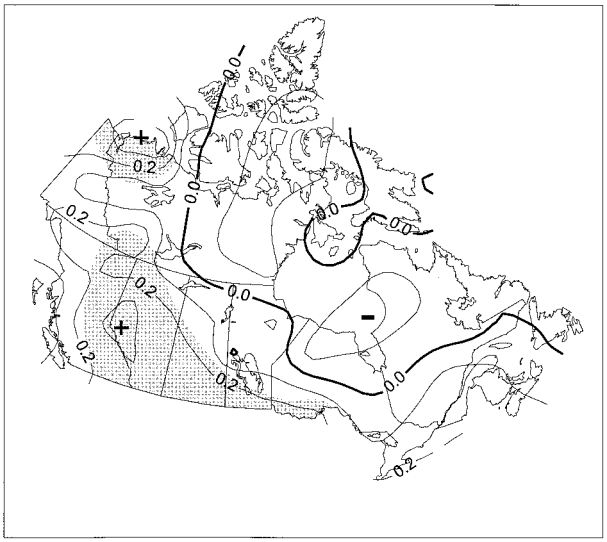

FIG. 6. Spatial distribution of the correlation coefficients between DJF SOI values and DJF standardized precipitation anomalies over Canada. Contour interval is 0.1. Shading denotes areas with correlation values significant at the 5% level as determined by the Monte Carlo procedure.

ada for the same periods as the composite analysis. Other seasonal SOI values were analyzed; however, the DJF season consistently showed the highest correlations with Canadian precipitation. The correlation values are mapped and tested for significance using the Monte Carlo procedure described in section 2b. The strongest results (i.e., several significant stations over a coherent region) occur with the contemporaneous DJF precipitation (Fig. 6). Significant positive correlation values extend from northern British Columbia and Alberta, across the south-central prairies, and into northwestern Ontario. A small region of the northwestern Arctic also shows significant results. Except for the northwestern Arctic and portions of northern British Columbia and Alberta, the correlations are statistically significant over much of the southern Canadian region defined previously. Even though the values are not very high (most of them are less than 0.3), they are significant at the 5% level based on a rigorous Monte Carlo procedure. This correlation pattern begins to emerge during the previous NDJ, is strongest during DJF and JFM, weakens during FMA, and disappears by MAM.

The lagged relationship is analyzed further by correlating the S0I values with areally averaged precipitation anomalies over the southern Canadian region (Fig. 7). The 5% significance level (as determined by the Monte Carlo procedure) is denoted by dashed lines. The significant contemporaneous winter correlation is

TABLE 3. Precipitation distribution over southern Canada for the JFM season following the onset of El Niño and La Niña events [JFM(+1)]. See text for definition of southern Canada.

Precipitation anomaly (mm)	El Niño events	La Niña events
−20 to −15	1911, 1930	None
−15 to −10	1914, 1925, 1957, 1958, 1972	None
−10 to −5	1926, 1939, 1976, 1986, 1991	1956
−5 to 0	1912, 1918, 1919, 1929, 1941, 1951, 1965, 1982	1917, 1928, 1988
0 to +5	1969	1916, 1924, 1964
+5 to +10	1953	1950, 1970, 1975
+10 to +15	None	1938, 1955, 1973
+15 to +20	None	1971

Driest 10% of all JFMs	Wettest 10% of all JFMs
1. 1912—El Niño	1. 1972—La Niña
2. 1993—Non-SO	2. 1953—Non-SO
3. 1931—El Niño	3. 1974—La Niña
4. 1915—El Niño	4. 1955—Non-SO
5. 1959—El Niño	5. 1936—Non-SO
6. 1981—Non-SO	6. 1935—Non-SO
7. 1973—El Niño	7. 1948—Non-SO
8. 1958—El Niño	8. 1939—La Niña

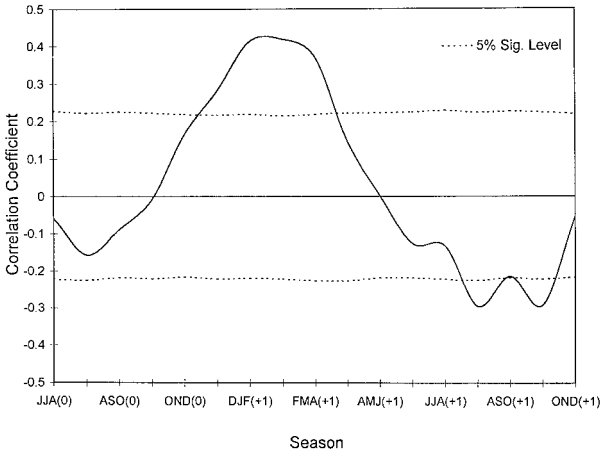

FIG. 7. Temporal distribution of the correlation coefficients between DJF SOI values and areally averaged precipitation anomalies over southern Canada. Dashed lines denote the 5% significance level as determined by the Monte Carlo procedure. Refer to Fig. 4 for definition of seasons.

clearly evident. In fact, the correlation associated with areally averaged precipitation increases to 0.42 in both DJF(+1) and JFM(+1). Following this, the values quickly diminish and reverse sign. During JAS(+1) and SON(+1), they become significantly negative. This is consistent with the time series of areally averaged precipitation anomalies (Fig. 4) that showed smaller positive (negative) anomalies associated with El Niño (La Niña) during late summer and early autumn of year +1. However, the composite analysis does not show any large-scale statistically significant responses during these periods. It is unclear from this analysis whether these smaller anomalies are SO related, a result of some other influence, or a manifestation of noise in the data.

Given that the nature of El Niño and La Niña events introduces a time lead in the precipitation field over Canada, the significant correlations in Fig. 7 suggest the possibility of developing a long-range forecasting technique for winter precipitation over southern Canada. A recent investigation by Stone et al. (1996) showed that the phase of the SOI can be used to make simple precipitation forecasts over various regions of the globe. Studies by Shabbar (1993) and Shabbar and Barnston (1996) indicated that the highest potential for predictability of precipitation in Canada is during winter. They also determined that the occurrence of the SO is a major contributor to this potential predictability.

The results of the correlation analysis between SOI and Canadian precipitation are consistent with those of the composite analysis for several reasons. First, the significant contemporaneous correlations indicate that the strongest precipitation responses coincide with the largest SOI values [which tend to occur during winter(+1) with respect to the onset of SO-related events] (e.g., Rasmusson and Carpenter 1982; Philander 1990). Second, the area covered by significant correlations in Fig. 6 corresponds closely to the area encompassed by significant values over southern Canada in the composite analysis. Finally, the significant positive correlation values indicate that El Niño events (negative SOI) are associated with negative precipitation anomalies and vice versa. This also implies that for the most part, winter(+1) precipitation over southern Canada is linearly related to the SO. The correlation analysis shows no other coherent areas with significant results. The north-central region of Canada (Fig. 3a) is not expected to show significant correlations with SOI, since it is only significantly related to the El Niño phase of the SO.

4) UPPER-ATMOSPHERIC CIRCULATION

Composite JFM(+1) 500-hPa anomalies associated with both El Niño and La Niña are presented in Figs. 8a and 8b. In the El Niño case, there is a deeper than normal Aleutian low, an amplification and eastward displacement of the western Canadian ridge, and negative height anomalies over the southeastern United States.

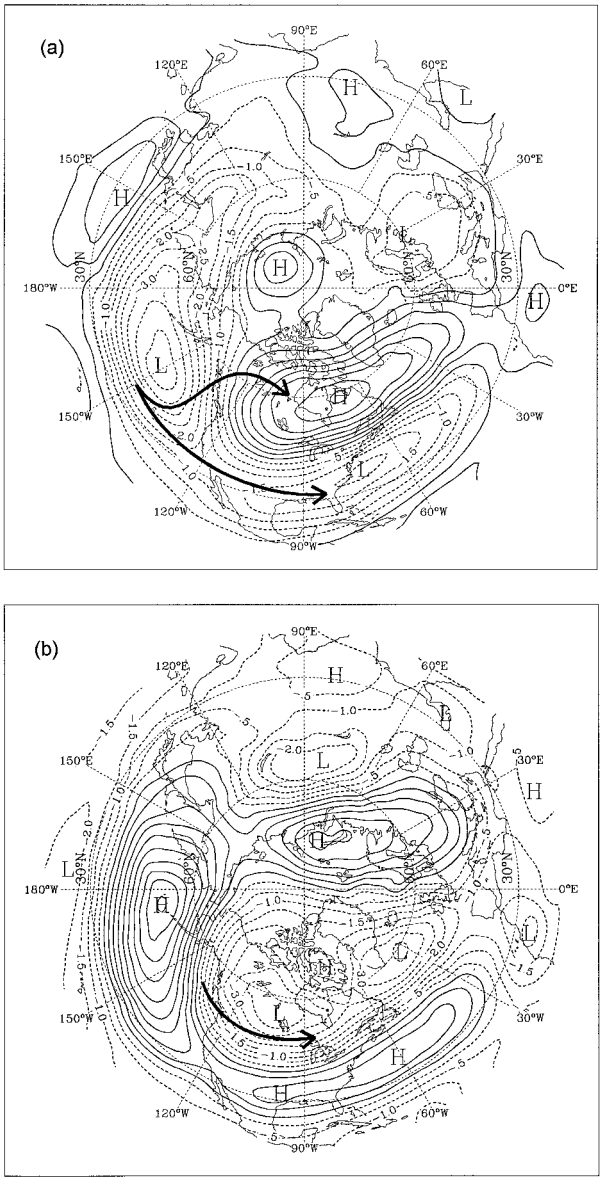

FIG. 8. (a) Composite 500-hPa anomalies (dam) for JFM(+1) associated with El Niño events. Contour interval is 0.5 dam. Negative contours are dashed. Arrows indicate approximate locations of the jet stream. (b) Same as (a) but for La Niña events.

This is similar to the positive phase of the PNA pattern that has often been associated with the winter following the onset of El Niño (e.g., Horel and Wallace 1981; Hamilton 1988). It also shows some characteristics of the tropical Northern Hemisphere (TNH) pattern (Barnston and Livezey 1987) that has also been associated with the JFM season following the onset of El Niño (Shabbar and Khandekar 1996). This upper-atmospheric flow pattern is likely associated with a split in the jet stream over North America (as denoted by arrows in Fig. 8a). A weaker branch would be diverted northward into the Northwest Territories, while the lower subtrop-

ical branch (whose mean position is over the Pacific Northwest and southwestern Canada) would be shifted several degrees of latitude southward. The southern Canadian region lies in between the two jets and, thus, would receive lower than normal precipitation.

Figure 8b essentially reveals an opposite circulation pattern associated with La Niña. This includes a weaker Aleutian low, an erosion and westward displacement of the western Canadian ridge, and positive height anomalies over the southeastern United States. This is similar to the negative phase of the PNA pattern that has often been associated with the winter following the onset of La Niña events (e.g., Emery and Hamilton 1985; Yarnal and Diaz 1986). The upper-atmospheric flow associated with this pattern would include stronger westerlies moving across the eastern Pacific and into southern Canada. The moist air originating from the Pacific would result in positive precipitation anomalies over southern Canada. The preceding has shown that the observed winter(+1) precipitation anomalies over southern Canada can be explained in terms of the associated upper atmospheric flow patterns. Furthermore, previous studies have indicated that similar flow patterns have often been directly associated with the different phases of the SO.

b. Winter(+1) positive precipitation anomaly over north-central Canada

In conjunction with the El Niño–related negative precipitation anomalies over southern Canada during winter(+1), an area of significant positive anomalies also exists to the north of this region (Fig. 3a). The positive anomalies are located over the southeastern portions of the Northwest Territories and extend into the northern prairies. This pattern first appears during DJF(+1), is strongest during JFM(+1), weakens during FMA(+1), and completely disappears by MAM(+1).

The degree of variability in the JFM(+1) areally averaged precipitation anomalies over north-central Canada associated with El Niño and non-SO periods is compared in Fig. 9. The distribution associated with El Niño covers a much smaller range. The average precipitation anomaly is greater than for non-SO; however, as with southern Canada, there is substantial overlap between El Niño and non-SO seasons. In fact, the entire El Niño distribution falls within the non-SO range indicating the influence of other factors on precipitation in this region. Due to a shorter period of record, the distributions are based on 52 yr of data that encompass 11 El Niño events. Of these 11 events, 9 are associated with positive anomalies and two of the four wettest JFM(+1) seasons on record are associated with El Niño.

As discussed previously, the composite JFM(+1) 500-hPa anomalies associated with El Niño (Fig. 8a) appear to be associated with a split jet stream over North America. The upper branch is diverted into the Northwest Territories, bringing moisture into this region, and thus partially explaining the observed positive precipitation anomalies. This area does not show significant negative anomalies during La Niña since the upper-atmospheric flow pattern (Fig. 8b) indicates a more zonal flow over Canada.

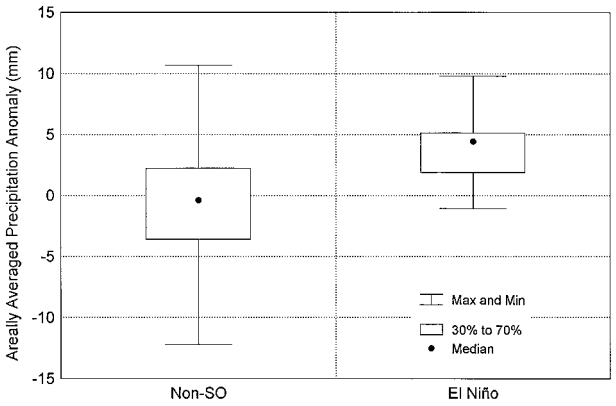

FIG. 9. Box plot comparing the JFM(+1) precipitation distribution for north-central Canada associated with El Niño and non-SO (non–El Niño and non–La Niña) periods. See text for definition of north-central Canada.

4. Discussion

A significant relationship between the SO and winter(+1) precipitation over southern Canada has been documented. These findings agree with the Canadian temperature study by Shabbar and Khandekar (1996), where the strongest temperature responses also occurred during the winter following the onset of both El Niño and La Niña events. However, there are also several differences. Shabbar and Khandekar (1996) determined a west to east progression of temperature anomalies for both El Niño and La Niña, starting in the autumn of the onset year and persisting through the following spring. No progression of precipitation anomalies was evident in this study. Furthermore, the areas encompassed by significant temperature anomalies were different from precipitation. Significant positive temperature anomalies extended from the Yukon, through the prairies, and into the Labrador coast in the warm phase; whereas, significant negative anomalies occurred mainly in the Yukon, British Columbia, and the Canadian prairies in the cold phase of the SO (see their Figs. 3 and 5). In this analysis, significant opposite responses were confined to the southern regions of Canada extending from British Columbia to the Great Lakes region. Moreover, another distinct response was determined for precipitation over north-central Canada associated with El Niño. Even though there are some similarities between SO-related temperature and precipitation responses over Canada, for the most part, they are notably different.

Several previous studies have indicated a general linear response between the different phases of the SO and temperature and precipitation over various regions of the globe (e.g., Yarnal and Diaz 1986; Ropelewski and

Halpert 1986, 1987, 1989; Bunkers et al. 1996). However, even in these analyses, the response to warm and cold events was not exactly opposite. Richman and Montroy (1996) examined composite January temperature and precipitation patterns over the United States and parts of Canada associated with El Niño and La Niña events. Their results strongly suggested that each type of event (i.e., El Niño versus La Niña) had its own unique characteristics in terms of temperature and precipitation, and the responses were not linear. Hoerling et al. (1997) suggested that the midlatitude atmospheric response to the different phases of the SO is inherently nonlinear, due to differences in the locations of intense tropical Pacific SST deep convection between El Niño and La Niña events. Due to the phase shift in the midlatitude atmospheric anomalies during the opposite phases of the SO, they concluded that midlatitude temperature and precipitation patterns should also have nonlinear relationships with the SO.

In this analysis, linearity is shown during winter(+1) over southern Canada. Even here, there are some differences in the areas of significant precipitation anomalies between El Niño and La Niña (Figs. 3a,b). In addition, the significant north-central Canadian response only occurs during El Niño events. A likely explanation for the nonlinear responses is that the upper-atmospheric flow patterns associated with each type of event is not exactly opposite (Hoerling et al. 1997). Therefore, the circulation dynamics associated with each of these flow patterns (which have a large influence on precipitation) are different. For example, the JFM(+1) composite 500-hPa anomaly patterns associated with El Niño and La Niña (Figs. 8a,b) have quite different dynamics associated with the flow. In El Niño situations, there is a split jet stream across North America. While north-central Canada receives positive precipitation anomalies, southern Canada has a deficit in precipitation. For La Niña, there is a strong jet stream through southern Canada. The precipitation response is, therefore, opposite in this region. Opposite responses are not observed in north-central Canada, since the dynamics of the flow are not conducive to negative precipitation anomalies in this region. The flow suggests near-normal precipitation.

This has been the first investigation to show significant SO-related impacts on precipitation over various regions of Canada. Previous global precipitation analyses have not shown significant precipitation anomalies over Canada for several reasons. Ropelewski and Halpert (1987, 1989), for example, fitted precipitation composites to a single 24-month idealized SO cycle that ran from July(−1) to June(+1). In their analysis, the first harmonic was extracted to determine large-scale regions of coherent responses with respect to the evolution of the SO episode. This assumes a general peak or trough during roughly half of the SO cycle. Due to the temporal smoothing inherent in their technique, short-lived (e.g., 3 to 4 month) SO-related impacts might not be detected.

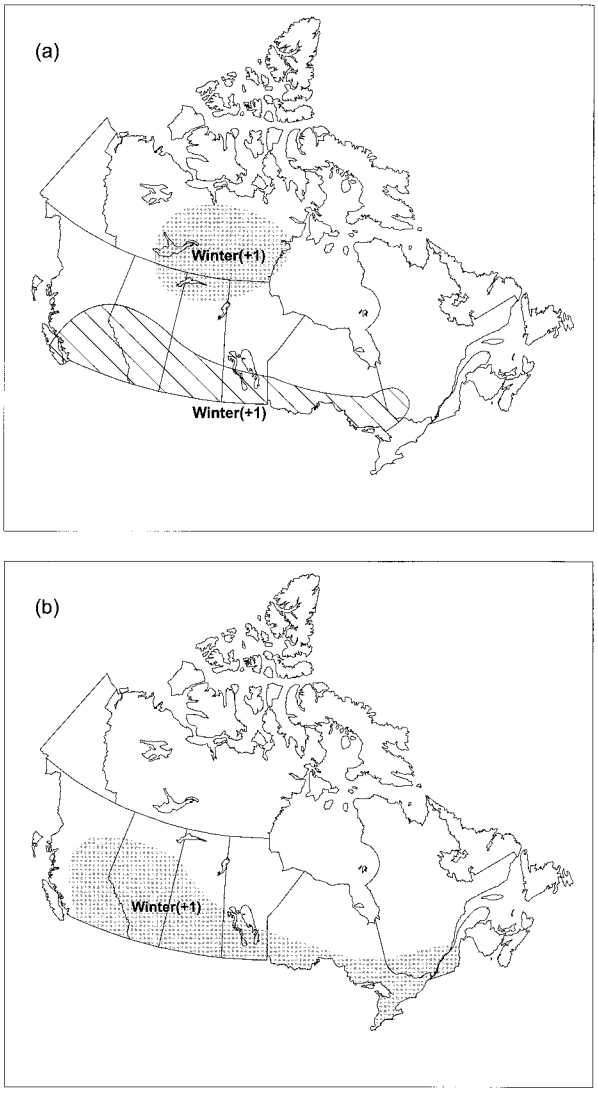

FIG. 10. (a) Schematic diagram showing the typical precipitation response over Canada associated with El Niño events. Drier than normal areas are hatched and wetter than normal areas are shaded. (b) Same as (a) but for La Niña events.

Our investigation examined the evolution of responses season by season from the El Niño/La Niña onset, to 3 yr following the onset, using both a composite and correlation analysis. As a result, this approach brings out regional details of the precipitation response not previously documented.

5. Summary and concluding remarks

This study provides a detailed analysis of the spatial and temporal behavior in precipitation responses over Canada, as they relate to the different phases of the SO. The typical responses are summarized in Figs. 10a and 10b. Two regions within Canada are found to be significantly influenced by El Niño events and one region

by La Niña events. All significant responses occur during the first winter following the onset of El Niño/La Niña events. The strongest results occur over an area that encompasses a large portion of southern Canada extending from British Columbia, across the prairies, and into the Great Lakes region. Here, both a composite and correlation analysis show significant negative (positive) precipitation anomalies associated with El Niño (La Niña) events. These precipitation anomalies can be explained by the associated 500-hPa anomalous circulation, which resembles the positive (negative) phase of the PNA pattern that has often been related to El Niño (La Niña) events. The significant precipitation response over north-central Canada associated with El Niño can also be explained by this upper atmospheric flow pattern.

In each of the outlined regions, the mean precipitation distribution associated with SO events is significantly different from non-SO periods. However, as revealed by Figs. 5 and 9, precipitation associated with individual El Niño and La Niña events shows considerable variability. Further analysis is required to determine the impact of El Niño and La Niña on the interannual variability in Canadian precipitation. Characteristics of individual events (e.g., intensity, duration, spatial extent), as well as more regional analyses of precipitation within Canada, may provide further insight. This study can, therefore, be considered as an initial step in identifying and understanding large-scale precipitation variability over Canada associated with the SO phenomenon. Given that the nature of SO events introduces a time lead in the precipitation field over Canada, the significant results shown here could aid in the development of a long-range forecasting technique for Canadian precipitation.

Acknowledgments. The authors would like to thank William Hogg, Xuebin Zhang, and Walter Skinner of the Atmospheric Environment Service for providing useful comments on an earlier version of the manuscript. We are also grateful to the three anonymous reviewers for their helpful suggestions on improving our paper.

APPENDIX

Wilcoxon Rank-Sum Test

The Wilcoxon rank-sum test (Bethea et al. 1995) determines the difference of means between two populations using ranked data. A *Z*-statistic is calculated from the following:

$$z = \frac{W_n - n_1(n_1 + n_2 + 1)/2}{[n_1 n_2 (n_1 + n_2 + 1)/12]^{1/2}},$$

where

n_1 = number of samples from population 1,

n_2 = number of samples from population 2,

W_n = the sum of the ranks of observations from population 1 in the ordered sample. Samples from populations 1 and 2 are combined, ordered (from smallest to largest), and assigned ranks (with 1 corresponding to the smallest value). W_n is the sum of the ranks from population 1.

The *Z*-statistic is used to test for statistical significance using the standard normal probability table. At the 5% significance level, there is a significant difference in the mean of the two samples if $Z < -1.96$ or $Z > +1.96$.

REFERENCES

Barnston, A. G., and R. E. Livezey, 1987: Classification, seasonality, and persistence of low-frequency circulation patterns. *Mon. Wea. Rev.,* **115,** 1083–1126.

Bethea, R. M., B. S. Duran, and T. L. Boullion, 1995: *Statistical Methods for Engineers and Scientists.* Marcel Dekker, 652 pp.

Bunkers, M. J., J. R. Miller, and A. T. DeGaetano, 1996: An examination of El Niño–La Niña related precipitation and temperature anomalies across the northern plains. *J. Climate,* **9,** 147–160.

Emery, W. J., and K. Hamilton, 1985: Atmospheric forcing of interannual variability in the northeast Pacific Ocean: Connection with El Niño. *J. Geophys. Res.,* **90,** 857–868.

Halpert, M. S., and C. F. Ropelewski, 1992: Surface temperature patterns associated with the Southern Oscillation. *J. Climate,* **5,** 577–593.

Hamilton, K., 1988: A detailed examination of the extratropical response to tropical El Niño/Southern Oscillation events. *J. Climatol.,* **8,** 67–86.

Hare, F. K., and M. K. Thomas, 1974: *Climate Canada.* Wiley Publishers, 256 pp.

Hoerling, M. P., A. Kumar, and M. Zhong, 1997: El Niño, La Niña, and the nonlinearity of their teleconnections. *J. Climate,* **10,** 1769–1786.

Horel, J. D., and J. M. Wallace, 1981: Planetary-scale atmospheric phenomena associated with the Southern Oscillation. *Mon. Wea. Rev.,* **109,** 813–829.

Khandekar, M. L., and V. R. Neralla, 1984: On the relationship between the sea surface temperatures in the equatorial Pacific and the Indian monsoon rainfall. *Geophys. Res. Lett.,* **11,** 1137–1140.

Kiladis, G. N., and H. F. Diaz, 1989: Global climatic anomalies associated with extremes of the Southern Oscillation. *J. Climate,* **2,** 1069–1090.

Livezey, R. E., and W. Y. Chen, 1983: Statistical field significance and its determination by Monte Carlo techniques. *Mon. Wea. Rev.,* **111,** 46–59.

McBride, J. L., and N. Nicholls, 1983: Seasonal relationships between Australian rainfall and the Southern Oscillation. *Mon. Wea. Rev.,* **111,** 1998–2004.

Mekis, E., and W. D. Hogg, 1996: Creation and analysis of daily precipitation time series. Atmospheric Environment Service Internal Rep., 40 pp. [Available from Atmospheric Environment Service, CARD, 4905 Dufferin Street, Downsview, ON M3H 5T4, Canada.]

Norman, G. R., and D. L. Streiner, 1986: *PDQ Statistics.* B. C. Decker, 172 pp.

Philander, S. G. H., 1990: *El Niño, La Niña, and the Southern Oscillation.* Academic Press, 289 pp.

Philips, D., 1990: *The Climates of Canada.* Environment Canada, 176 pp.

Rasmusson, E. M., 1984: El Niño: The ocean/atmosphere connection. *Oceanus,* **27,** 5–12.

——, and T. H. Carpenter, 1982: Variations in tropical sea surface

temperature and surface wind fields associated with the Southern Oscillation/El Niño. *Mon. Wea. Rev.,* **110,** 354–384.

Richman, M. B., and D. L. Montroy, 1996: Nonlinearities in the signal between El Niño/La Niña events and North American precipitation and temperature. Preprints, *13th Conf. on Probability and Statistics in the Atmospheric Sciences,* San Francisco, CA, Amer. Meteor. So., 90–97.

Rogers, J. C., 1988: Precipitation variability over the Caribbean and tropical Americas associated with the Southern Oscillation. *J. Climate,* **1,** 172–182.

Ropelewski, C. F., and M. S. Halpert, 1986: North American precipitation and temperature patterns associated with El Niño/Southern Oscillation (ENSO). *Mon. Wea. Rev.,* **114,** 2352–2362.

——, and ——, 1987: Global and regional scale precipitation patterns associated with El Niño/Southern Oscillation. *Mon. Wea. Rev.,* **115,** 1606–1626.

——, and P. D. Jones, 1987: An extension of the Tahiti–Darwin Southern Oscillation index. *Mon. Wea. Rev.,* **115,** 2161–2165.

——, and M. S. Halpert, 1989: Precipitation patterns associated with the high index phase of the Southern Oscillation. *J. Climate,* **2,** 268–284.

Shabbar, A., 1993: Potential predictability of precipitation in Canada. Canadian Climate Centre, AES, Rep. 93-8, 26 pp. [Available from Atmospheric Environment Service, 4905 Dufferin Street, Downsview, ON M3H 5T4, Canada.]

——, and A. G. Barnston, 1996: Skill of seasonal climate forecasts in Canada using canonical correlation analysis. *Mon. Wea. Rev.,* **124,** 2370–2385.

——, and M. Khandekar, 1996: The impact of El Niño–Southern Oscillation on the temperature field over Canada. *Atmos.–Ocean,* **34,** 401–416.

Stone, R. C., G. L. Graeme, and T. Marcussen, 1996: Prediction of global rainfall using phases of the Southern Oscillation index. *Nature,* **384,** 252–255.

Wheaton, E. E., L. M. Arthur, B. Chorney, S. Shewchuck, J. Thorpe, J. Whiting, and V. Wittrock, 1992: The prairie drought of 1988. *Climate Bull.,* **26,** 188–205.

Yarnal, B., and H. F. Diaz, 1986: Relationships between extremes of the Southern Oscillation and the winter climate of the Anglo-American Pacific coast. *J. Climatol.,* **6,** 197–219.